CrystEngComm

Accepted Manuscript

ROYAL SOCIETY OF CHEMISTRY

www.rsc.org/crystengcomm

Studies on Polymorph Conversion in a New Cyclodextrin Inclusion Compound

José A. Fernandes,* Ana I. Ramos, Paulo Ribeiro-Claro, Filipe A. Almeida Paz and Susana S. Braga*

A novel β-cyclodextrin (βCD) inclusion compound was prepared using 4-phenylpyridine N-oxide (PPNO) as the organic guest. The inclusion compound, βCD · PPNO, was characterised both in solution and the solid state using numerous techniques. ^{1}H NMR in aqueous solution allowed the determination of a 1:1 stoichiometry and an association constant of 164±21 M^{-1}. Powder and single-crystal X-ray diffraction studies evidenced the formation of two distinct crystal phases, appearing at different timings. Over time, one of the crystal phases converts spontaneously into the other. This work is the first to monitor the conversion of different polymorphs of cyclodextrin inclusion compounds in real time.

Introduction

The concept of Secondary Building Unit (SBU) as a rigid, chemically-stable entity used as a large building block for the synthesis of Metal-Organic Frameworks (MOFs), has been introduced by Yaghi's group and developed gracefully by the group of Férey. The modular preparation of MOFs from SBUs relies either on the formation of chemical bonds between individual units or by way of employing a bridging ligand to establish the connections. In most of the commonly employed SBUs, the exterior layer of bridging ligands surrounding the inner (unsaturated) metallic core is composed of simple ditopic molecules.

For the last several years, we have been particularly interested in the preparation of MOFs using either new ligands,[1-7] or by employing the modular construction with Secondary Building Units (SBU).[8, 9] Some of us have also developed a line concerning

the preparation and characterisation of inclusion compounds from cyclodextrins.[10-16] By combination of the two skills we have prepared the inclusion compound of 4,4'-biphenyldicarboxilic acid into β-cyclodextrin (βCD),[17] which was aimed at being used as a bulkier bridging ligand, *i.e.*, a purely organic SBU. Cyclodextrins (CDs) are a well-known family of cyclic oligosaccharides with the shape of a truncated cone (Fig. 1a) and a hydrophobic cavity able to host guest molecules of suitable size and geometry to form inclusion compounds.[18-20] CDs are often used as drugs carriers for improved bioavailability, since they can change the guest's physico-chemical parameters: stability, solubility, and/or dissolution rate.[19, 20] Aromatic organic compounds are particularly suitable guests due to the excellent docking abilities of the apolar aromatic ring, by establishing hydrophobic interactions with the host cavity. The pyridine-N-oxide moiety, present in 4-phenylpyridine N-oxide (PPNO) (Scheme 1b), is of pharmacologic relevance, comprising the central skeleton of the vasodilating drug minoxidil and occurring in a plethora of new drug candidates. Pyridine-N-oxide derivatives with kinase-3β inhibiting action are currently under study for the treatment of a wide range of disfunctions, including diabetes, schizophrenia, or malaria infections.[21, 22] 4-nitropyridine-N-oxide fights *Pseudomonas aeruginosa* by reducing biofilm formation and quorum sensing,[23] and several picryl amino pyridine N-oxides have antimicrobial and antifungal action.[24] Pyridine-N-oxides from *Allium stipitatum* are bioactive: the anti-inflammatory properties of pyrithione and a few dithio-pyridine N-oxides were demonstated,[25] and, on the new dithio compounds, antimicrobial (against *Mycobacterium* and *Staphylococcus* strains) and antitumoral actions (on MCF7 breast carcinoma and A549 lung carcinoma) were found.[26] A number of pyridine-N-oxide compounds display antiviral features: one class proved suitable for treating feline coronavirus and viruses linked to SARS (severe acute respiratory syndrome),[27] and another is associated with inhibition of HIV replication.[28, 29] A series of pyridinyloxy(thio)phenyl plant growth regulators has also been developed. [30]

The present work describes the inclusion of PPNO into βCD, which is, *a priori,* expected to occur since the aromatic moieties of PPNO provide a good docking site for βCD and furthermore the molecular recognition of PPNO by a calix[4]pyrrole derivative has been previously reported.[31] Characterisation results will demonstrate that inclusion takes place *via* the interaction of the host's hydroxyl groups with the terminal N-O moiety of the guest. The affinity and stoichiometry of the inclusion complexation in aqueous solution were studied by ^{1}H NMR spectroscopy; the solid inclusion

compound was also prepared and was characterised in detail using in tandem several solution and solid-state techniques. Depending on the crystallisation times, two different solid fractions can be isolated, each containing different proportions of two distinct polymorphs. While the faster crystallising Fraction A is rich in the polymorph *P*1, coined as I, the slow crystallising fraction B is rich in the polymorph C2, coined as II. The *P*1 structure readily converts into the *C*2 structure, either by mechanical action (*e.g.*, grinding) or by undergoing a spontaneous phase transition over time (between 2 and 4 days). This transformation was unequivocally observed by monitoring the powder X-ray diffractograms of fractions of the inclusion compound βCD·PPNO over time (see dedicated section below), and the structure of each polymorph was described using single-crystal diffraction studies. Noteworthy, this report constitutes the first detailed study of a structural transformation of this kind for CD inclusion compounds.

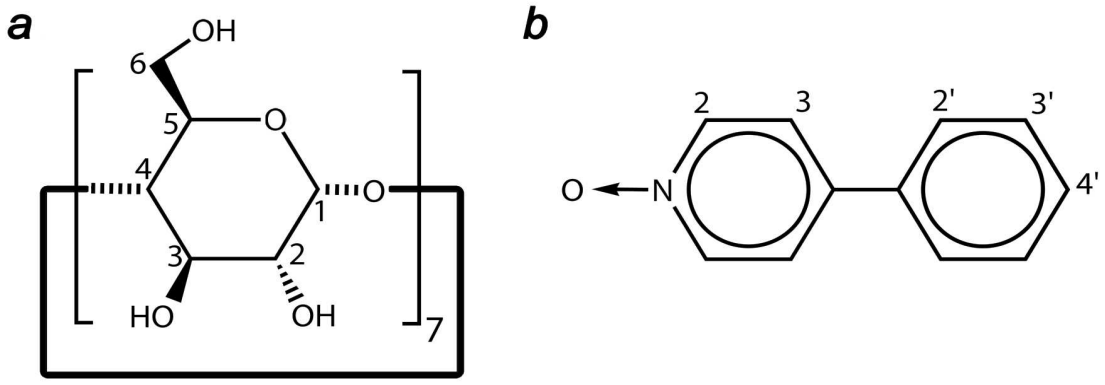

Fig. 1 Molecular structure and ^{1}H labeling of **(a)** βCD and **(b)** PPNO.

Results and discussion

Aims and scope

We aim to prepare novel organic SBUs based on inclusion compounds of βCD following the design strategy and chemical principles presented in our previous and recent work.[17] The approach starts by the selection of the reagents, in which βCD is the obvious candidate as host given its rigid geometry, size and predictability of the crystal packing.[17] PPNO was chosen as guest because it combines several important physical and chemical features: i) its shape is ideal for inclusion into βCD, following

the several examples of biphenyl derivates,[32-34] and the formation of the inclusion of PPNO into calyx[4]pyrrol;[31] ii) *N*-oxides have been employed in the construction of coordination polymers,[35-38] being thus good candidates for the preparation of organic SBUs. iii) the bioactivity of the pyridine *N*-oxide compounds makes PPNO a good starting material for the construction of pharmacologically relevant MOFs.

In order to better study the inclusion phenomenon of *N*-oxide molecules and to have a firm control over the experimental procedure, a stepwise aproach was employed. PPNO, producing only discrete molecules upon reaction with metals, was selected as the monotopic ligand. The present work reports the results we have obtained from the first step (CD inclusion), namely: *i*) the determination of stoichiometry and constant of formation in solution state; *ii*) characterisation in the solid state, including the structure of the two polymorphs by the conjugation of crystal data and theoretical calculations. Finally, we comment the observation of the spontaneous transformation of one of the polymorphs into the other.

Inclusion complexation in solution

Stoichiometry determination

The first set of solutions for ^{1}H NMR studies were prepared according to the continuous variation method (Job plot).[39] In this methodology, solutions of host and guest are mixed in varying molar fractions while keeping constant the sum of their concentrations (see details in the dedicated Experimental Section) and the variations in the chemical shifts of their protons ($\Delta\delta$) relative to those of the pure solutions are registered. The plot maximum corresponds to the preferred stoichiometric proportion of βCD and PPNO in the inclusion compound (in aqueous solution).[40]

The six βCD protons were monitored and the variations in their chemical shift in function of the molar fraction are represented in Figure 2. The variations of the guest (PPNO) ^{1}H resonances were was very small and highly affected by the experimental error of the method, thus being omitted for clarity.

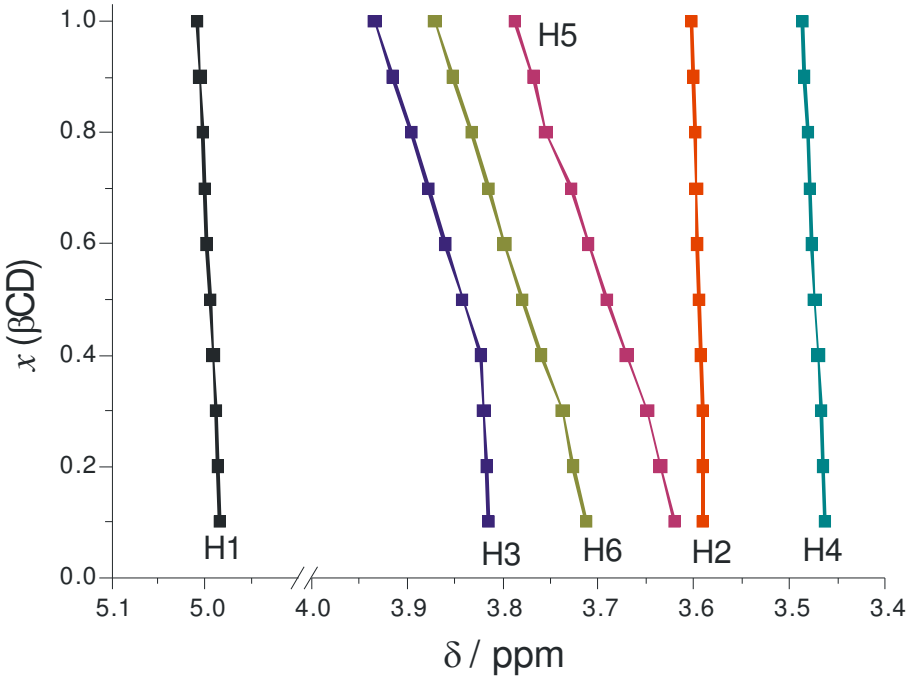

Figure 2. Chemical shift variation for each βCD ^{1}H while performing the continuous variation method: [βCD] + [PPNO] = 10 mM. See Figure 1 for the ^{1}H labeling scheme. Full lines connecting the experimental points are for indicative purposes only.

Because H3 and H5 are located inside the βCD cavity they are the most sensitive to guest inclusion and, thus, expected to exhibit higher chemical shifts upon changes on the cavity´s environment. In the collected experimental data, H5 showed the highest chemical shift variation[40] and so it was selected for the Job plot representation depicted in the Figure 3. The maximum for this plot was achieved at 0.5, thus indicating that the preferred stoichiometry for inclusion compound in solution is 1 : 1.

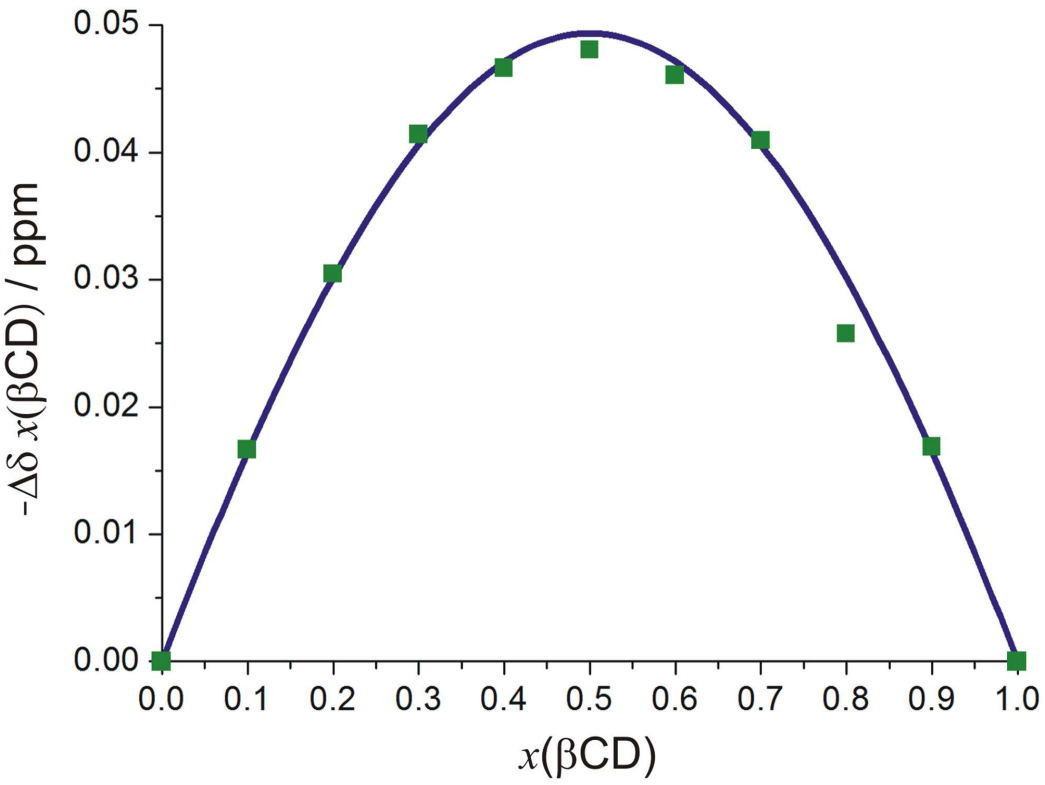

Figure 3. Job plot of H5 for the inclusion of PPNO into βCD (in D_2O). The line corresponds to a calculated curve using the apparent formation constant for a 1 : 1 inclusion compound.

Determination of the Apparent Association Constant

For the calculation of the apparent association constant (K_{app}) the dataset from the Job plot was complemented with a new data set. These new samples comprised a fixed volume of the PPNO solution and variable volumes the solution of βCD (and adjusting the final volume to 700 μL with D_2O, see Experimental Section for further details). The range of monitored concentrations was chosen according to Fielding's studies.[40] Note that the two data sets were used in the calculation of the value of the constant, in a total of 16 experimental data points which were treated by a curve fitting method.[17, 40] The Fielding method postulates that, knowing the complex stoichiometry, experimental data are comparable to a binding isotherm. $\Delta\delta_{max}$ (the maximum variation of the ^1H chemical shift of a hypothetical solution of pure inclusion compound in relation to the pure βCD solution) and K_{app} are the set variables solved iteratively until the best fit to the data points is achieved, as depicted in Figure 4.

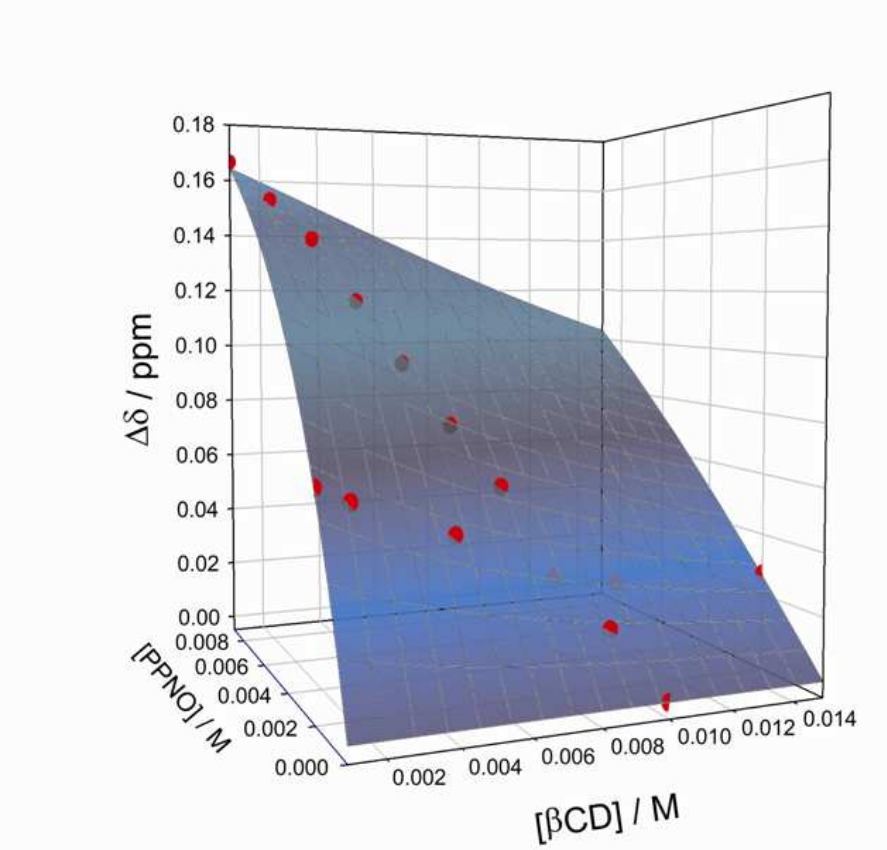

Figure 4. Comparison between the experimental data (red dots) and the calculated binding isotherm for K_{app} determination.

Numerical treatment of this data set affords the K_{app} and $\Delta\delta_{max}$ values of 164±21 M^{-1} and 0.283±0.017 ppm, respectively. The value of the formation constant may appear somewhat low when compared to reported constants of several inclusion compounds in βCD.[41, 42] Nevertheless, it must be stressed that most of these arise from other techniques, and that "the equilibrium constants determined by different experimental methods for the same reaction can significantly deviate from one another" (Rekharsky and Inoue, 1998).[41] Regarding the inclusion complexes studied by NMR, the lowest reported value was found for the βCD·8-aniline-1-naphtalene-sulfonate complex (K_{app} = 71 M^{-1}).[41] K_{app} for βCD·PPNO finds some similarity with the complex βCD·(*R*)-1,1′-binaphthyl-2,2′-diylphosphate (K_{app} = 263 M^{-1}), and the values are slightly higher for the complexes βCD·(*S*)-1,1′-binaphthyl-2,2′-diylphosphate (K_{app} = 346 M^{-1})[41] and βCD·*p*-hydroxybenzaldehyde (K_{app} = 3–4 × 10^2 M^{-1})[43] (we note that the K_{app} for the later complex was calculated by us using the exact same experimental procedure). The mild host-guest affinity in βCD·PPNO may mean that this complex has insufficient

stability for use as an SBU in the production of MOFs. Nonetheless, solid-state spectroscopic and crystallographic studies were carried out to evaluate the formation and stability of this host-guest system as a solid compound.

Inclusion of PPNO into βCD by co-crystallisation

Preparation and preliminary examination of the solids

Crystals of βCD · PPNO were obtained by the aqueous co-dissolution of the components (βCD and PPNO) in the 1 : 1 stoichiometric proportion (as determined from the solution studies), followed by slow cooling to ambient temperature approximately 24 h. Then, a first batch of crystals was isolated (fraction A) and the mother liquour was allowed to rest at room temperature for the development of more crystals for 2-4 days, after which fraction B was collected. These fractions were found in a later stage to correspond to different proportions of two polymorphs of the same inclusion compound (with the same empirical formula). The results obtained by elemental analysis confirmed a 1 : 1 stoichiometry for both fractions, further pointing to the presence of *ca.* ten hydration water molecules per adduct unit. Inclusion compound formation was further confirmed by thermogravimmetric analysis (TGA), collected for a sample pertaining to fraction B (see Figure S1 in the ESI). Furthermore, this technique has revealed the loss of only 8 water molecules per complex unit in the sample, which is ascribed to partial dehydration after prolonged storage at ambient conditions.

The samples were also studied by FT-IR spectroscopy, with fractions A and B being, as expected, indistinguishable by this technique. The presence of the guest was confirmed by observation of some of its vibrational modes. Furthermore, some bands had maxima slightly shifted in comparison to those of pure PPNO as listed in Table S1 on the ESI. These changes are coherent with the inclusion of PPNO into the cavity of βCD.

$^{13}C\{^{1}H\}$ CP/MAS NMR

The spectrum of fraction B was collected and compared to those of the starting materials, PPNO and βCD, as depicted in Figure 5. The spectrum of βCD hydrate exhibits the typical multiple sharp resonances for each carbon atom associated with

small variations in local environments.[44-46] Upon inclusion of PPNO the resonance multiplicity and structure is generally reduced and, noteworthy, host carbons occur as singlets (with small shoulders in the case of C_1 and C_4). These spectral features are in close relation with the formation of βCD dimers by hydrogen bonding involving the C_2 and C_3 hydroxyl groups, located at the wider rim of the host. This geometry, described in the crystallographic and theoretical sections, affords an overall symmetrysation of the host macrocycle, evidenced by resonance reduction in the solid-state $^{13}C\{^1H\}$ NMR spectra.

Guest resonances are also observed in the spectra of fraction B, with a strong modification on the pattern of chemical shifts, thus strongly supporting encapsulation of PPNO inside the cavity of βCD.

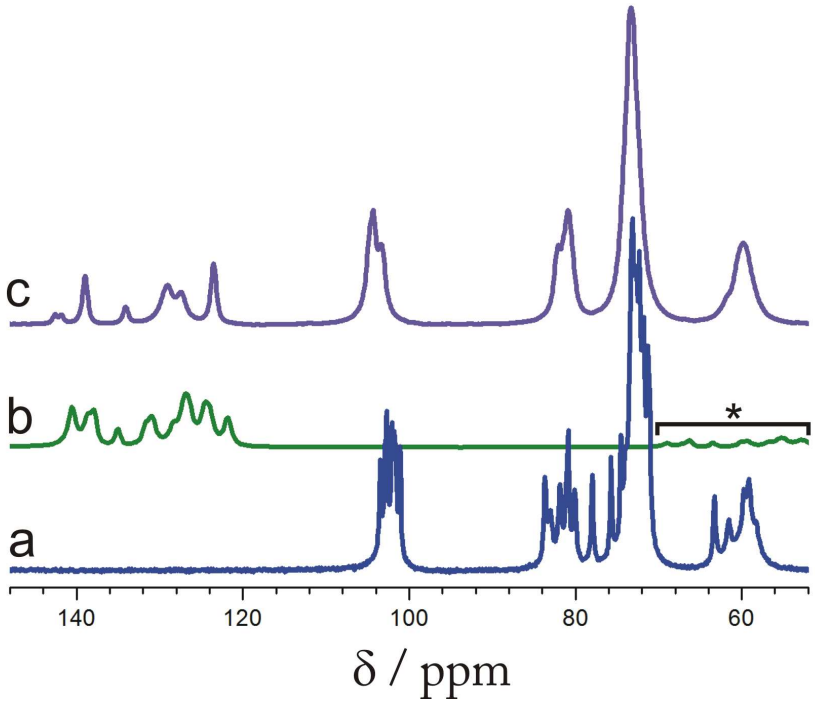

Figure 5. $^{13}C\{^1H\}$ CP/MAS NMR spectra of (**a**) βCD, (**b**) PPNO and (**c**) fraction B of βCD·PPNO. The formation of the adduct reduces the multiplicity of the host signals and modifies the pattern of the guest signals. Spinning side bands are assigned with an asterisk.

Powder X-ray diffraction

The powder X-ray diffraction patterns of fractions A and B are provided in Figure 6. Fraction A, formed directly from the reaction mixtures after 1 day, was found to be essentially formed by crystals of a phase coined as I. Fraction B, collected after several days of crystallisation in a desiccator, was conversely found to be rich in a compound which is hereafter coined as II. The milling at room temperature of fraction A samples converts phase I into II (details below, in a dedicated subsection), and for this reason, to obtain powdered material for analysis, the crystals of both phases had to be ground at low temperature by using liquid nitrogen.

Some batches obtained from the synthesis were found to correspond to pure phases, showing diffraction patterns similar to models described in the review of Caira.[47] These models are grouped in several classes, and it is straightforward to say that phases I and II correspond to the general classes 12 and 11 of Caira's article, respectively. Each of these classes corresponds to a specific crystal packing of the hosts, and to specific unit cell parameters, which were ultimately confirmed by single-crystal X-ray diffraction as detailed in the following subsection. In this context, in phase I we expect to observe the host dimers forming a supramolecular packing named "intermediary packing" in which the cavities are isolated from each other, while in phase II the cavities of the host should be instead aligned in a "channel packing".

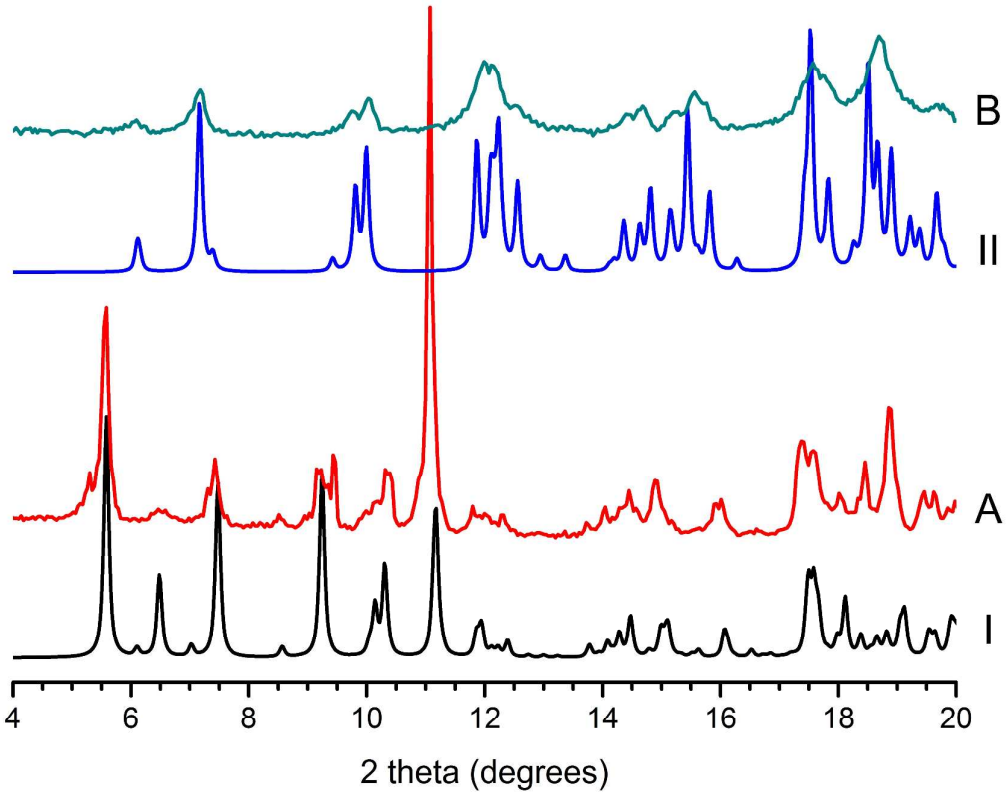

Figure 6. Powder X-ray diffraction patterns of fractions A and B, obtained by grinding the samples in liquid nitrogen. The patterns for phase I and II, depicted for comparison purpose, were calculated using the programme Mercury CSD version 3.3.[48]

Single-crystal X-ray diffraction

After a careful inspection of the two isolated fractions (A and B), single-crystals suitable for X-ray analyses could be directly isolated and separated using an optical microscope, and their structure was determined (experimental details in Table 1, dedicated subsection below and Figure 7.).

The crystal structure of phase I is described by a triclinic unit cell (space group *P*1) containing a whole dimer of βCD with two PPNO guests inside the formed cavity. The dimer, as usual, is packed head-to-head. As derived from the powder X-ray diffraction studies the dimers of βCD are indeed packed via the so-called "intermediary packing" which means that the tails of βCD molecules are not aligned, avoiding the formation of channels. The two guests are highly disordered, with their phenyl rings forming a π-π interaction with distance between centromers of 3.716(13) Å, and the N-oxide moieties interacting with water molecules. There are 22 water molecules per unit cell disordered

over 32 different crystallographic locations distributed as follows: 6 sites (with 4.1 water molecules) permit the interaction with N-oxide moieties from the guests; 15 locations (with 8.8 water molecules) correspond to intermolecular interstices; 12 sites (with 9.1 water molecules) allow hydrogen bonding bridges between adjacent tails of βCD. Noteworthy, this does not occur in phase II as detailed below. A search for solvent accessible voids, using the programme PLATON[49], revealed no voids capable of containing additional water molecules.

Phase II belongs to the monoclinic space group *C*2, with the β-CD dimer being formed by two symmetric hosts related by a C_2 axis. The supramolecular packing of the dimers forms channels with head-to-head and tail-to-tail interactions between the macromolecules (the head corresponds to the hydroxyl groups in positions 2 and 3 and the tail to the hydroxyl groups in position 6). There are about 9 water molecules per asymmetric unit, distributed over 18 locations. While one half of a water molecule is interacting with an N-oxide moiety inside the cavity, the remaining 8.5 are in the interstices between the hosts. Apparently, no water molecule is located in the alignment of head-to-head or tail-to-tail supramolecular interactions. The pair of guests located inside the cavity is disordered in two locations with equal occupancies. While the phenyl rings have a π-π interaction at a distance of 3.755(6) Å (distance between centromers), the N-oxide moieties present a distance of ca. 3.50 Å between the oxygen atoms. Additionally, the N-oxide moieties form hydrogen bond interactions with one water molecule and at least one hydroxyl moiety from the hosts. If defects in the crystals are not counted, the disordered locations of the guests are mutually excluded by molecular superimposition. This means that the location of one guest molecule in the channel defines the location of its neighbours, and this ordering extends to the whole channel. This order among the guests do not respect the overall symmetry elements (C_2 axes) to which the hosts are subjected. The overall disorder is present in the crystal because there is no contact between the channels, which makes the orientations of the guests randomly distributed, when different channels are compared. Once more, there is no void space in the structure capable of containing further solvent molecules.

Table 1. Crystal and structure refinement data for βCD·PPNO·xH_2O

	Phase I	Phase II
Formula	$C_{106}H_{202}N_2O_{94}$	$C_{106}H_{194}N_2O_{90}$
Formula weight	3008.68	2936.62
Crystal system	Triclinic	Monoclinic
Space group	*P*1	*C* 2
a/Å	15.281(3)	18.7766(6)
b/Å	15.431(3)	24.6489(8)
c/Å	17.911(4)	15.3471(5)
α/º	99.573(9)	—
β/º	113.073(9)	109.642(2)
γ/º	102.518(10)	—
Volume/Å^3	3641.9(13)	6689.7(4)
Z	1	2
D_c/g cm^{-3}	1.372	1.458
μ(Mo-Kα)/mm^{-1}	0.122	0.129
Crystal size/mm	0.16×0.04×0.04	0.20×0.16×0.10
Crystal type	Colourless Needle	Colourless Prism
θ range	3.53 to 25.35	3.55 to 29.13º
Index ranges	$-13 \le h \le 18$	$-25 \le h \le 24$
	$-18 \le k \le 14$	$-33 \le k \le 33$
	$-21 \le l \le 21$	$-21 \le l \le 21$
Reflections collected	31719	52904
Independent reflections	18955	9998
Completeness to θ_{max}	97.1%	99.6 %
Final *R* indices [I>2σ(I)][a,b]	*R*1 = 0.1384	*R*1 = 0.688
	*wR*2 = 0.3494	*wR*2 = 0.1592
Final *R* indices (all data)[a,b]	*R*1 = 0.1808	*R*1 = 0.1439
	*wR*2 = 0.3831	*wR*2 = 0.1970
Weighting scheme[c]	*m* = 0.2000	*m* = 0.0957
	n = 0.0000	*n* = 5.7869
Largest diff. peak and hole	1.292 and –1.668 eÅ^{-3}	0.840 and -0.713 eÅ^{-3}

[a] $R1 = \sum \| |F_o| - |F_c| \| / \sum |F_o|$; [b] $wR2 = \sqrt{\sum \left[w\left(F_o^2 - F_c^2\right)^2 \right] / \sum \left[w\left(F_o^2\right)^2 \right]}$

[c] $w = 1/\left[\sigma^2\left(F_o^2\right) + \left(mP\right)^2 + nP \right]$ where $P = \left(F_o^2 + 2F_c^2\right)/3$

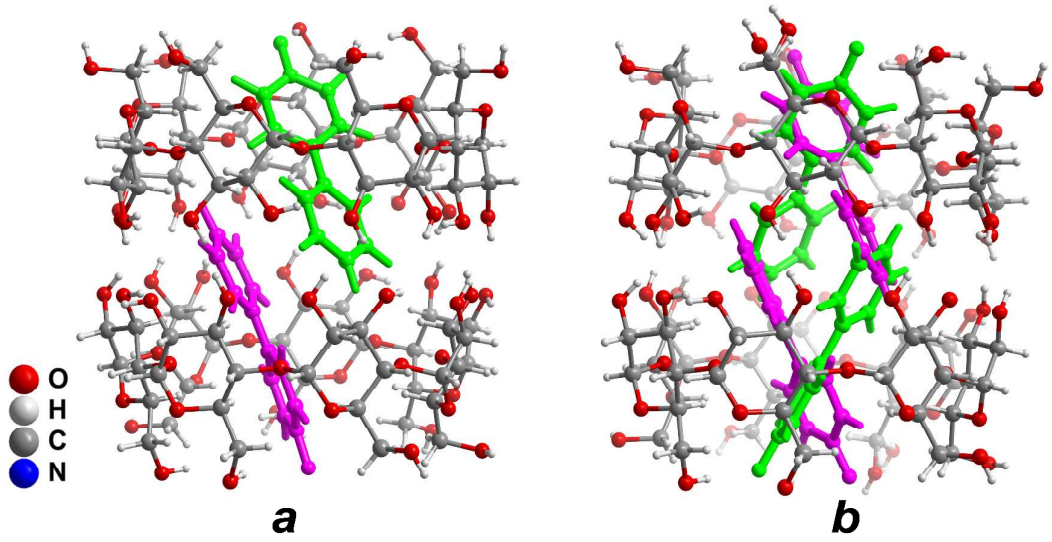

Figure 7. Schematic representation of the cyclodextrin dimers present in the crystalline structures of the two phases of βCD·PPNO: (**a**) The β-CD dimer of phase I is composed by two unequivalent hosts and two unequivalent and highly disordered guests represented in green and magenta for clarity. (**b**) The βCD dimer of phase II is composed by two symmetry related βCD·PPNO pairs. The guest is disordered in two locations with equal occupancies (represented in green and magenta for clarity). The figure has been prepared by using the programme Diamond, Version 3a.[50]

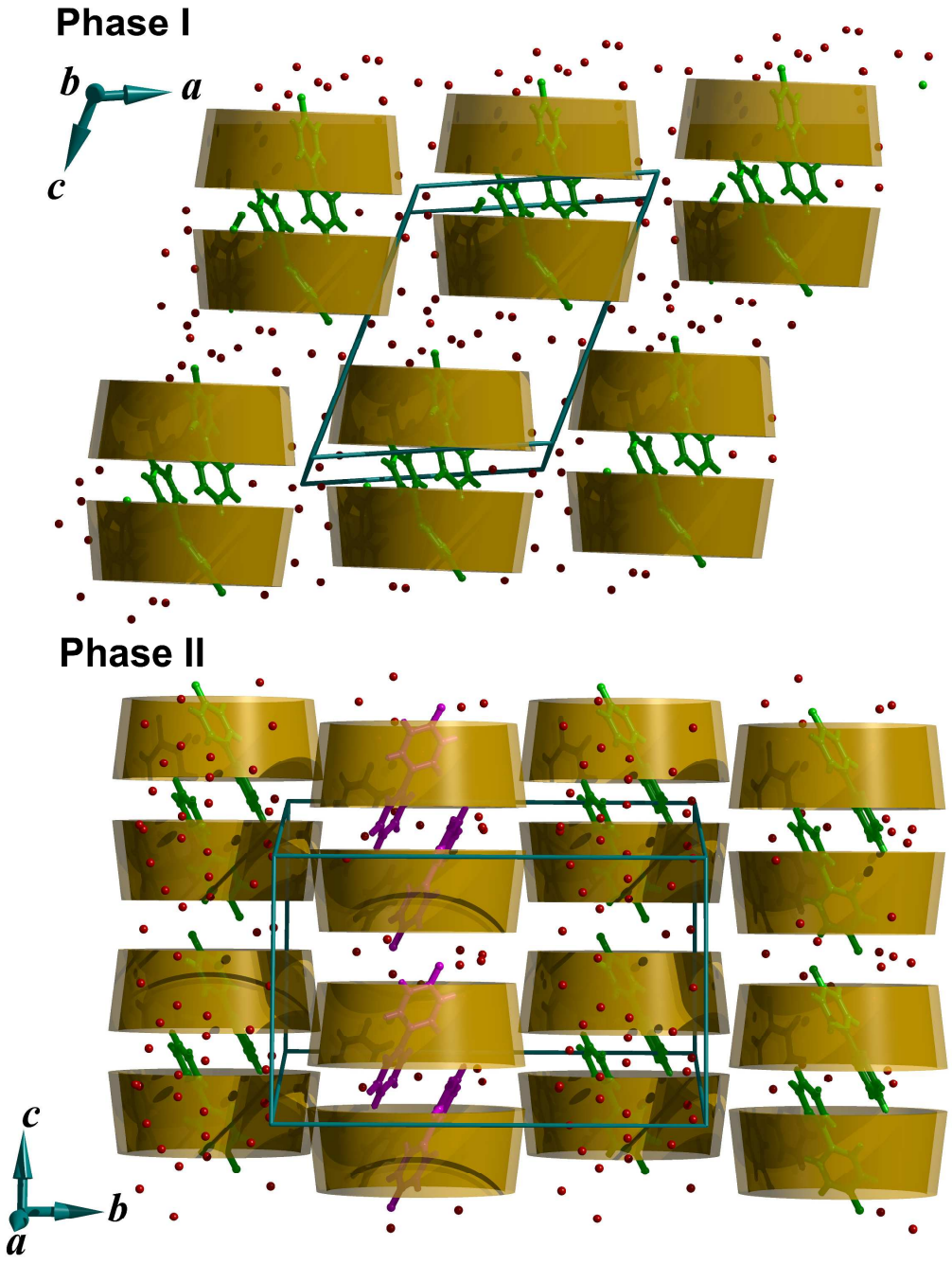

Figure 8. Crystal packing of the two phases of βCD·PPNO. The cyclodextrin molecules are depicted as truncated cones located around the geometrical centres of the crystallographic entity. Phase I comprises an "intermediary packing" in which the dimers of βCD do not merge into channels. In opposition, the cavities of βCD in phase II are aligned and form the so-called "channel packing". The guests are distributed randomly on the two crystallographic sites depicted in two different colours. In each channel, every molecule PPNO determinates the conformation of its neighbours. The figure has been prepared by using the programme Diamond, Version 3a[50] and exported to POV-Ray[51] where the cyclodextrin molecules were replace by truncated cones with similar dimensions.

Conversion of polymorph I into polymorph II

During the development of this work the two abovementioned phases were identified as two different polymorphs of the same inclusion compound. In the case of CD inclusion complexes, there are some examples of polymorphs to consider, namely with βCD complexes of methylparaben,[52] barbital,[53] and benzoic acid.[54] The latter, reported by T. Aree et al, presents striking similarities with the results of this work, since it also formed initially a triclinic *P*1 phase (I) which converts over time to a monoclinic *C*2 phase (II); however, the phase conversion in the crystals of with βCD·benzoic acid has seemingly taken a longer time (phase II crystals were serendipitously observed and identified after one and a half year).[54] Remarkably, we have also serendipitously discovered the conversion between the two phases upon repeating, after several weeks, the data collection of powder X-ray diffraction of the same sample. Further investigation has demonstrated that the samples identified as phase I transformed into phase II material either spontaneously or by mechanochemical induction, and that the transition is irreversible. We should note that while phase I is the crystal which forms essentially overnight after slow cooling of the reaction mixture, pure crystals of the phase II only appear after slow evaporation of the solvent. As far as our knowledge goes, the interconversion between different polymorphs of cyclodextrin inclusion compounds was only previously observed once, by T. Aree *et al*.[54] These findings can be supported by Ostwald's law of stages, in the view of polymorphism, stating that the least stable crystal form is likely to crystallise first.[55, 56] The conversion of phase I into phase II has been observed by two ways: *i*) Spontaneous conversion, monitored in the bulk sample, by powder X-ray diffraction (Fig. 9) or by single-crystal X-ray diffraction when a specific crystal clearly indexed as belonging to phase I was indexed as a low crystallinity phase II two days later; ii)Crystals of phase I transform into crystals of phase II in a few days, with this phenomenon being followed by powder X-ray diffraction (Fig. 11) *ii*) Induced conversion, by milling of crystals of phase I for about one minute at ambient temperature to produce a phase II powder (Fig. 10)

We found that the only way to obtain ground samples of powders rich in phase I was to immerse them with liquid nitrogen during the grinding. However, the reduction of particle size in these samples induces an expectable phase transition, and indeed after 24

hours they had fully transformed into phase II. For this reason, the monitoring of the spontaneous phase conversion by PXRD was only possible with non-ground samples, presenting a high level of preferential orientation as seen in Figure 11.

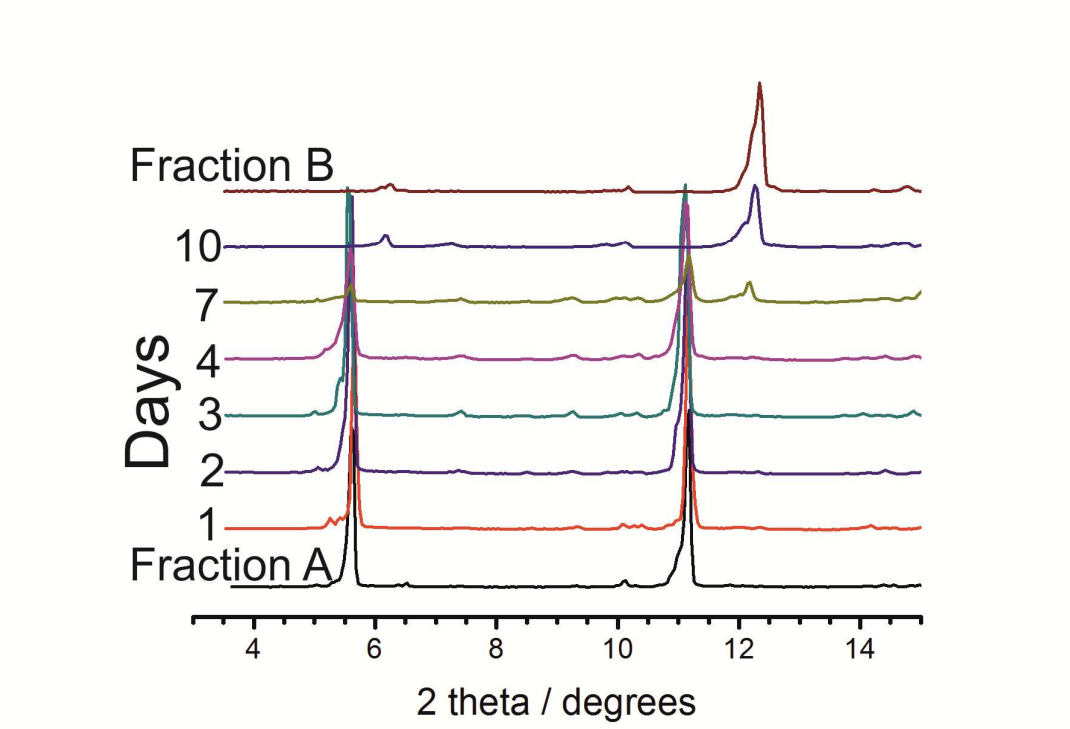

Figure. 9 Kinetic study of the spontaneous conversion between phases. A sample of fraction A comprising almost pure phase I was submitted to repeated diffractograms during a period of 10 days. In spite of the strong incidence of preferential orientation peaks, it is possible to observe the phase transition, which occurs between the 4^{h} and 10^{th} days. A difractogram of non-ground fraction B is presented for comparison purpose only.

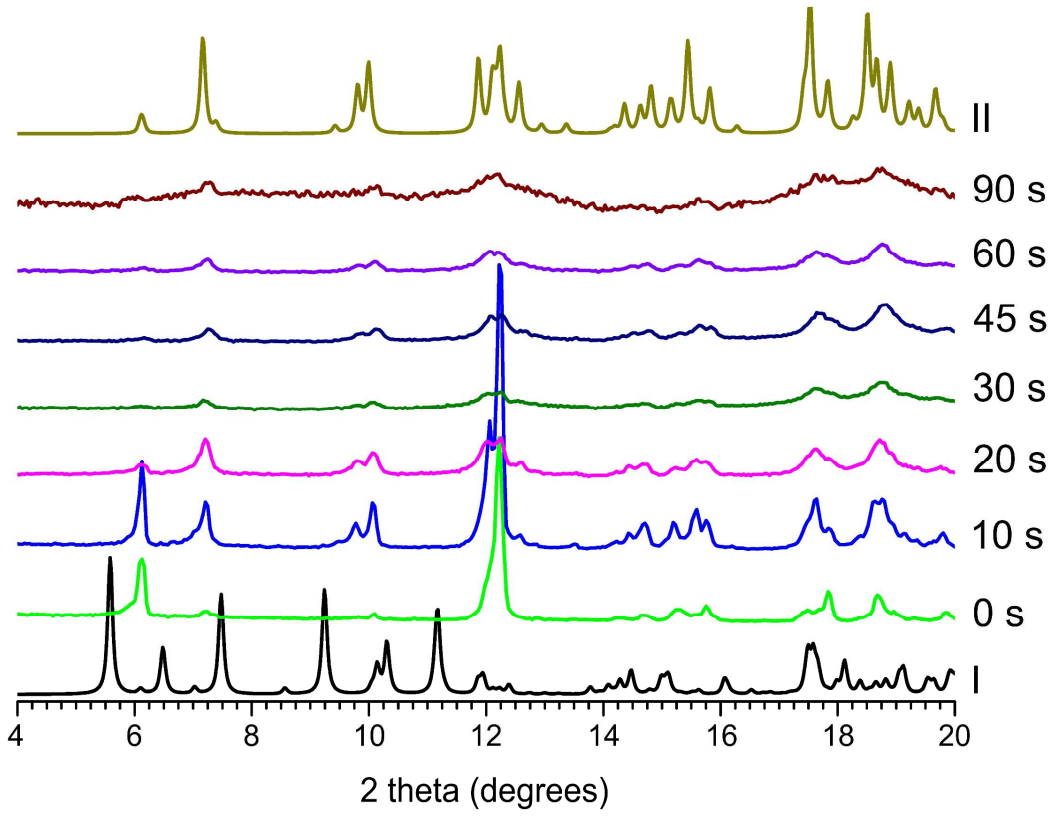

Figure. 10 Kinetic study of the phase conversion induce by mechanical grinding. A sample of fraction A comprising almost pure phase I was submitted to repeated diffractograms with small intervals of grinding. The overall time of grinding is seen at the right side of the diffractograms. Calculated patterns for phases I and II are also depicted for comparison. The patterns for low griding times are dominated by an intense peak corresponding to preferential orientation.

As described in the crystallographic section, the crystals of phase I present high disorder in the overall structure, with particularly strong incidence in the water molecules. Additionally, the packing forces between different layers in I depend on bridges formed by the water molecules. These two factors allow the motion of the layers and thus contribute for the conversion of phase I into phase II. In phase II the waters are less disordered, and also, the packing of the βCD dimers in infinite channels leads to a stabilised structure in which the water molecules have a smaller contribution for the packing forces.

Concluding remarks

The inclusion complexation of βCD with phenylpyridine N-oxide was studied both in aqueous solution and in the solid state and found to occur with the same stoichiometry (1:1) in these two states. This is not a rare feature in βCD inclusion compounds (examples: methyl- and propyl-paraben,[57] 2,4-dichlorophenoxyacetic acid),[58] but a few exceptions have also been reported, namely with the guests *p*-hydroxybenzaldehyde[43] and β-naphthyloxyacetic acid.[59] A value of 164 M^{-1} for the apparent formation constant, determined by numerical methods using adequate NMR data, is considered a low value, and apparently the complex is not stable enough for serving, in future work, as an organic SBU for the preparation of coordination polymers.

The preparation of the βCD·PPNO inclusion compound in the solid state lead to the isolation of two distinct polymorphs, each occurring at a different crystallisation time, and one of them being more stable, as predicted by Ostwald's law. The crystals which form in short time (24h), deemed as form I, are metastable and tend to evolve in time, transforming into the stable form II crystals in a matter of two to four days. The remarkable aspects of this work were that the conversion between phases could be monitored both by means of single-crystal diffraction for isolated crystals and by powder X-ray diffraction for the bulk material and, furthermore, that these techniques have demonstrated that the conversion occurs either spontaneously within a few days, or faster, upon mechanical induction (by milling the crystals in a mortar).

Acknowledgements

We acknowledge Fundação para a Ciência e a Tecnologia (FCT), European Union, QREN, European Fund for Regional Development (FEDER), through the programme COMPETE, for general funding to QOPNA (project PEst C-QUI/UI0062/2013; FCOMP-01-0124-FEDER-037296) and CICECO (PEst C-CTM/LA0011/2013), and for specific funding toward the purchase of the single-crystal X-ray diffractometer. The FCT and the European Social Fund are acknowledged for grant SFRH/BPD/63736/2009 (to JAF).

Experimental

Materials and methods

βCD was kindly donated by Laboratoires La Roquette (France) and PPNO (98%) was purchased from Sigma-Aldrich.

Microanalyses for CHN were performed at University of Aveiro (Department of Chemistry) on a LECO CHNS-932 Elemental Analyser. Samples were combusted at 1000 ºC for 3 min with helium as the purge gas.

Attenuated Total Reflection Fourier Transform Infrared (ATR-FTIR) spectra were acquired on a Mattson 7000 FTIR spectrometer equipped with a Specac Golden Gate Mk II ATR accessory having a diamond top-plate and KRS-5 focusing lens (resolution 2.0 cm^{-1}; 32 scans per spectrum).

FT-IR spectra (range 4000–350 cm_1) were collected as KBr pellets using a Bruker Tensor 27 spectrometer by averaging 128 scans at a maximum resolution of 2 cm^{-1}.

Thermogravimmetric analyses (TGA) were performed on a Shimadzu TGA-50 thermogravimetric analyser, from room temperature to *ca.* 600 ºC, using a heating rate of 5 ºC min^{-1}, under a static air atmosphere, with a flow rate of 20 mL min^{-1}. The sample holder was a 5 mm (platinum plate and the sample mass was about 10 to 15 mg.

Powder X-ray diffraction (XRD) data were collected at the Central Laboratory for Analysis (University of Aveiro) on an X'Pert MPD Philips diffractometer (Cu Kα X-radiation, λ=1.54060 Å), equipped with an X'Celerator detector, a curved graphite-monochromated radiation and a flat-plate sample holder, in a Bragg-Brentano para-focusing optics 15 configuration (40 kV, 50 mA). Intensity data were collected in continuous scanning mode in the ca. $3^{o} \leq 2\theta \leq 50^{o}$ angular range.

^{1}H NMR solution spectra were recorded on a Bruker CXP 300 spectrometer. Chemical shifts were quoted in parts per million from tetramethylsilane. Spectra recorded in D_2O were referenced to HOD at δ=4.79 ppm.[60]

$^{13}C\{^{1}H\}$ CP/MAS NMR spectra were recorded at 125.72 MHz on a Bruker Avance 500 spectrometer, with an optimized π/2 pulse for ^{1}H of 4.5 μs, 2 ms contact time, a spinning rate of 9 kHz and 12 s recycle delays. Chemical shifts are quoted in parts per million from tetramethylsilane.

Job Plot

The stoichiometry of β-CD·PPNO in deuterium oxide solution was determined using the continuous variation method or Job's method.[39] This method involves running a series of experiments varying the host to guest concentrations while keeping their sum constant ([βCD] + [PPNO]), at well defined *r* values (*r* = [β-CD]/{[β-CD] + [PPNO]}). In particular, 10 mM fresh D_2O solutions of PPNO and β-CD were mixed (i) to constant volume, *i.e.*, the sum of the initial concentrations of β-CD and PPNO remained equal to 10 mM, and (ii) to defined values of *r*, where *r* took values from 1/10 to 9/10, in steps of 1/10. The stoichiometry was finally determined by plotting Δδ·[β-CD] against *r*, where Δδ is the NMR shift of the proton of β-CD with the largest Δδ (which was H5 – see Figure 3), and finding the *r* value corresponding to the maximum of this distribution.

Determination of the Apparent Formation Constant

Five NMR samples were prepared, each containing [PPNO]=2 mM and [β-CD]=1, 2, 5, 10 and 15 mM. The determination of K_{app} was performed by the least-squares fitting of the observed Δδ of H5 (of the host) to the following equations using 16 data points (The five with [PPNO]=2 mM referred above plus the eleven from the Job plot):[17, 40]

$$\Delta = \left(K_1 H_{0i} - K_1 G_{0i}\right)^2 + 2K_1 H_{0i} + 2K_1 G_{0i} + 1$$

$$[HG]_i = \frac{\left(K_1 H_{0i} + K_1 G_{0i} + 1\right) - \sqrt{\Delta}}{2K_1} \qquad \text{(Eq. 1)}$$

$$\Delta\delta_{obs,i} = x_{HG,i}\Delta\delta_{max} = \frac{[HG]_i}{H_{0i}}\Delta\delta_{max} \qquad \text{(Eq. 2)}$$

H corresponds to the host (βCD), G to the guest (PPNO) and HG to the inclusion compound. G_{0i} and H_{0i} corresponds to the initial concentrations at each data point. The molar fraction x_{HG} is the fraction of HG with respect to the total amount of H. The Δδ quantities correspond to the variation of chemical shifts with respect to a solution of pure host, where $\Delta\delta_{obs,i}$ corresponds to the observed values and $\Delta\delta_{max}$ is the hypothetical variation for a pure 1 : 1 inclusion compound for the chosen proton (H5). The data fit, determination of associated errors (Table 2) and Figure 4 were produced by using SigmaPlot, version 11, from Systac Software Inc.

Table 2. Relevant values for the fit in the determination of K_{app}

K_{app}	164±21 M^{-1}
$\Delta\delta_{max}$	0.283±0.017 ppm
Standard deviation	0.0029 ppm
R^2	0.997

Preparation of the βCD · PPNO inclusion compound

An aqueous solution (2.0 mL) of βCD (0.384 g, 0.292 mmol) was treated stepwise with solid PPNO (0.050 g, 0.292 mmol) and the resulting solution was kept at 60 ºC for 30 minutes under strong stirring. Crystallisation was achieved by placing the resulting solution in a Dewar container with a water bath at 80 ºC and allowing it to cool slowly. Greyish-white crystals formed in solution after one day (fraction A).

The remaining mother liquour was kept in a desiccator and monitored for the formation of new crystals over a period of roughly two weeks (fraction B). Anal. Calc. for ($C_{42}H_{70}O_{35}\cdot$ $C_{11}H_9ON\cdot 10H_2O$) (1486.33): C, 42.83; H, 6.71; N, 0.94%; Found: C, 42.71; H, 6.96; N, 0.96%. ATR-IR (cm^{-1}): $\bar{\nu}$ = 3272 m, 2923 m, 2894 m, 2360 w, 2184 w, 2007 w, 1646 w, 1509 w, 1475m, 1413 w, 1369 m, 1330 m, 1299 w, 1232 w, 1155 m, 1101 m, 1079 m, 1022 vs, 998 vs, 935 m, 844 m, 752 m, 725 m, 684 m, 646 m, 605 m, 572 s, 526 m, 474 m, 443 m, 410 m, 352 m, 332 m, 302 m, 285 m. ^{13}C CP/MAS NMR (9 kHz, 25 ºC, ppm): δ=142.6 (PPNO, C_{quat}), 141.9 (PPNO, C_{quat}), 139.0 (PPNO, C_2), 134.1 (PPNO, $C_{4'}$), 129.0 and 127.5 (PPNO, $C_{2',3'}$), 123.5 (PPNO, C_3), 104.4 (β-CD, C_1), 80.9 (β-CD, C_4), 73.3 (β-CD, $C_{2,3,5}$), 59.8, (β-CD, C_6) ppm.

Solid state studies

Generally, peaks of phase II in the unground samples were undetectable in some samples and visible as smaller peaks in others. Figure 10 depicts the variation of patterns with grinding. While for some samples 30 seconds of milling were enough for eliminate any trace of phase I, for others, the conversion was only considered to be complete after 60 seconds of grinding.

The kinetic study depicted in Figure 9 was performed by determining the diffractogram

of the same sample of crystals corresponding to fraction A. The sample was not ground to avoid the fast conversion of phase I to phase II. The conversion was considered to be complete after 10 days.

In order to avoid the conversion between phases, the diffractograms depicted in Figure 6 were obtained from powders ground during immersion on liquid nitrogen.

Single-Crystal X-ray Diffraction Studies

Suitable colourless single-crystal of the two phases were manually harvested and immediately immersed in FOMBLIN Y. Then, they were mounted on a Hampton Research CryoLoop with the help of a Stemi 2000 stereomicroscope equipped with Carl Zeiss lenses.[61] Data were collected on a Bruker X8 Kappa APEX II CCD area-detector diffractometer (Mo Kα graphite-monochromated radiation, λ = 0.71073 Å) controlled by the APEX2 software package[62] and equipped with an Oxford Cryosystems Series 700 cryostream monitored remotely using the software interface Cryopad.[63] Images were processed using the software package SAINT+,[64] and data were corrected for absorption by the multi-scan semi-empirical method implemented in SADABS.[65]

The structure was solved using the direct methods implemented in *SHELXS-97*.[66, 67] which allowed the immediate location of the CD molecules. All remaining non-hydrogen atoms were located from difference Fourier maps calculated from successive full-matrix least-squares refinement cycles on F^2 using *SHELXL-97*. [67, 68]

Both structures contained some special features that had to be treated carefully: i) the CD units had disorder in some CH_2OH groups; ii) A large number of atoms in phase I and some in phase II needed to be treated with command ISOR in order to reduce their anisotropy; iii) Inspite of being easily located from difference Fourier maps, the guest molecules in the structure of phase I needed to be isotropically refined by using the constrains for hexagonal shape (AFIX 66) for the phenyl moieties; iv) All the water molecules were refined isotropically with a common ADP, and free occupancies; v) In following refinements the occupacies of water molecules were fixed, taking in account their value obtained by the free refinement and geometrical concerns about the overall occupancies of clusters of water sites.

Hydrogen atoms bound to carbon and oxygen atoms were placed at their idealised positions using the *HFIX* instructions (43 aromatic, 23 methylen, 13 ring and 83 for hydroxyl groups). All these hydrogen atoms were included in the final structural

model in riding-motion approximation with isotropic thermal displacement parameters fixed at 1.2×U_{eq} (for C) or 1.5×U_{eq} (for O) of the atom to which they are attached. This step resulted in several close contacts between the hydrogen atoms. Thus, a considerable number of contact restrains were added to the refinenment with the code DFIX, by forcing H…H distances to be larger than 2.10 and 2.40 Å for intra- and extramolecular contacts, respectively. The final refinements of the structures converged to solutions in which the highest difference peak, and deepest hole are 1.292 and -1.668 e A^{-3}, respectively for I, and 0.840 and -713 e A^{-3}, respectively for II.

Crystallographic data collection and structure refinement details are summarized in Table 1. CCDC 1027505 and 1027506 contain the supplementary crystallographic data for this paper for I and II, respectively. These data can be obtained free of charge from The Cambridge Crystallographic Data Centre via www.ccdc.cam.ac.uk/data_request/cif.

Notes and references

QOPNA (Research Unit on Organic Chemistry, Natural and Agroalimentary Products), Department of Chemistry, CICECO, University of Aveiro, 3810-193 Aveiro, Portugal. Fax: +351 234 401470; Tel:+351 234 401418;
*E-mail: sbraga@ua.pt, jafernandes@ua.pt

1. S. M. F. Vilela, J. A. Fernandes, D. Ananias, L. D. Carlos, J. Rocha, J. P. C. Tomé and F. A. A. Paz, *CrystEngComm*, 2014, **16**, 344-358.
2. S. M. F. Vilela, D. Ananias, P. Silva, M. Nolasco, L. D. Carlos, V. d. Z. Bermudez, J. Rocha, J. P. C. Tomé and F. A. A. Paz, *CrystEngComm*, 2014, **16**, 8119-8137.
3. S. M. F. Vilela, D. Ananias, J. A. Fernandes, P. Silva, A. C. Gomes, N. J. O. Silva, M. O. Rodrigues, J. P. C. Tomé, A. A. Valente, P. Ribeiro-Claro, L. D. Carlos, J. Rocha and F. A. A. Paz, *J. Mater. Chem. C*, 2014, **2**, 3311-3327.
4. B. Monteiro, J. A. Fernandes, C. C. L. Pereira, S. M. F. Vilela, J. P. C. Tomé, J. Marçalo and F. A. Almeida Paz, *Acta Cryst. B*, 2014, **70**, 28-36.
5. S. M. F. Vilela, R. F. Mendes, P. Silva, J. A. Fernandes, J. P. C. Tomé and F. A. A. Paz, *Cryst. Growth Des.*, 2013, **13**, 543-560.
6. P. Silva, J. A. Fernandes and F. A. Almeida Paz, *J. Chem. Crystallogr.*, 2013, **43**, 165-170.
7. F. A. Almeida Paz, J. Klinowski, S. M. F. Vilela, J. P. C. Tomé, J. A. S. Cavaleiro and J. Rocha, *Chem. Soc. Rev.*, 2012, **41**, 1088-1110.

8. J. Rocha, F. A. A. Paz, F. N. Shi, R. A. S. Ferreira, T. Trindade and L. D. Carlos, *Eur. J. Inorg. Chem.*, 2009, 4931-4945.
9. F. A. A. Paz, J. Klinowski, S. M. F. Vilela, J. P. C. Tomé, J. A. S. Cavaleiro and J. Rocha, *Chem. Soc. Rev.*, 2012, **41**, 1088-1110.
10. S. S. Braga, I. S. Gonçalves, E. Herdtweck and J. J. C. Teixeira-Dias, *New J. Chem.*, 2003, **27**, 597-601.
11. F. A. Almeida Paz and S. S. Braga, in *Organometallic Compounds: Preparation, Structure and Properties.*, ed. H. F. Chin, Novascience publishers, Hauppauge, NY, 2010, pp. 465-481.
12. A. I. Ramos, T. M. Braga, P. Silva, J. A. Fernandes, P. Ribeiro-Claro, M. F. S. Lopes, F. A. A. Paz and S. S. Braga, *CrystEngComm*, 2013, Accepted for publication.
13. A. I. Ramos, T. M. Braga, J. A. Fernandes, P. Silva, P. J. Ribeiro-Claro, F. A. A. Paz, M. F. S. Lopes and S. S. Braga, *J. of Pharmaceut. Biomed.*, 2013, **80**, 34-43.
14. J. Marques, T. M. Braga, F. A. A. Paz, T. M. Santos and S. S. Braga, *Biometals*, 2009, **22**, 541-556.
15. S. Bruno, J. A. Fernandes, J. Marques, S. C. Neto, P. J. Ribeiro-Claro, M. Pillinger, F. A. A. Paz, M. P. M. Marques, S. S. Braga and I. S. Gonçalves, *Eur. J. Inorg. Chem.*, 2011, 4955-4963.
16. J. A. Fernandes, S. Lima, S. S. Braga, M. Pillinger, P. J. Ribeiro-Claro, J. E. Rodriguez-Borges, A. D. Lopes, J. J. C. Teixeira-Dias and I. S. Gonçalves, *Organometallics*, 2005, **24**, 5673-5677.
17. J. A. Fernandes, F. A. A. Paz, S. S. Braga, P. J. Ribeiro-Claro and J. Rocha, *New J. Chem.*, 2011, 1280-1290.
18. K. Yannakopoulou and I. M. Mavridis, *Curr. Org. Chem.*, 2004, **8**, 25-34.
19. T. Loftsson and D. Duchane, *Int. J. Pharm.*, 2007, **329**, 1-11.
20. J. Szejtli, *Chem. Rev.*, 1998, **98**, 1743-1853.
21. P. R. Angibaud, L. F. Marconnet-Decranne and J. Arts, *New pyridine or pyrimidine derivatives useful for treating proliferative diseases e.g. cancer, psoriasis, rheumatoid arthritis, atherosclerosis, restenosis, Crohn's disease, allergic rhinitis, cardiac dysfunction, Parkinson's diseases. European Patent EP1979327-A1, Janssen Pharmaceutica N.V. (JANC)* 2007.
22. L. F. Marconnet-Decranne, S. F. Gaurrand and P. R. Angibaud, *New pyridine and pyrimidine derivatives useful for the treatment of e.g. proliferative diseases such as cancer. European Patent EP1979326-A1, Janssen Pharmaceutica N.V. (JANC)* 2008.
23. N. Vanoyan, S. L. Walker, O. Gillor and M. Herzberg, *Langmuir*, 2010, **26**, 12089-12094.
24. D. H. Badgujar, M. B. Talawar, S. N. Asthana and P. P. Mhulikjar, *Indian J. Chem.*, 2010, **49B**, 1675-1677.
25. P. Krejčová, P. Kučerová, G. I. Stafford, A. K. Jäger and R. Kubec, *J. Ethnopharmacol.*, 2014, **154**, 176-182.
26. O'Donnell, R. Poeschl, O. Zimhony, M. Gunaratnam, J. B. C. Moreira, S. Neidle, D. Evangelopoulos, S. Bhakta, J. P. Malkinson, H. I. Boshoff, A. Lenaerts and S. Gibbons, *J. Nat. Prod.*, 2009, **72**, 360-365.
27. J. Balzarini, E. Keyarts, L. Vijgen, F. Vandemeer, M. Stevens, E. D. Clercq, H. Egberink and M. V. Ranst, *J. Antimicrob. Chemoth.*, 2006, **57**, 472-481.
28. J. Balzarini, M. Stevens and D. Schols, *J. Antimicrob. Chemoth.*, 2005, **55**, 135-138.

29. M. Stevens, C. Pannecouque, E. D. Clercq and J. Balzarini, *Biochem. Pharmacol.*, 2006, **71**, 1122-1125.
30. R. Henrie, C. M. Green and R. E. Sticker, *New N-phenyl N'-(pyridinyl-N-oxide) urea cpds. useful as plant growth regulators, e.g. for retarding senescence and increasing yield in soybean. United States Patent US4787931-A, FMC Corporation*, 1988.
31. B. Verdejo, G. Gil-Ramírez and P. Ballester, *J. Am. Chem. Soc.*, 2009, **131**, 3178-3179.
32. P. Giastas, K. Yannakopoulou and I. M. Mavridis, *Acta Cryst. B*, 2003, **59**, 287-299.
33. T. J. Brett, J. J. Stezowski, S. Liu and P. Coppens, *Chemical Commun.*, 1999, 551-552.
34. Y. Liu, Y.-L. Zhao, H.-Y. Zhang and H.-B. Song, *Angew. Chem. Int. Ed. Engl.*, 2003, **42**, 3260-3263.
35. S. C. Manna, E. Zangrando, J. Ribas and N. R. Chaudhuri, *Dalton Trans.*, 2007, 1383-1391.
36. D. G. Mantero, A. Neels and H. Stoeckli-Evans, *Inorg. Chem.*, 2006, **45**, 3287-3294.
37. R. Sarma, A. K. Boudalis and J. B. Baruah, *Inorg. Chim. Acta*, 2010, **363**, 2279-2286.
38. J. J. Zhang, Y. Zhao, S. A. Gamboa and A. Lachgar, *Cryst. Growth Des.*, 2008, **8**, 172-175.
39. P. Job, *Ann. Chim. France*, 1928, **9**, 113-203.
40. L. Fielding, *Tetrahedron*, 2000, **56**, 6151-6170.
41. M. V. Rekharsky and Y. Inoue, *Chem. Rev.*, 1998, **98**, 1815-1917.
42. M. Fujiki, T. Deguchi and I. Sanemasa, *Bull. Chem. Soc. Jpn.*, 1988, **61**, 1163-1167.
43. S. S. Braga, T. Aree, K. Imamura, P. Vernut, I. Boal-Palheiros, W. Saenger and J. J. C. Teixeira-Dias, *J. Incl. Phenom. Macro.*, 2002, **43**, 115-125.
44. R. P. Veregin, C. A. Fyfe, R. H. Marchessault and M. G. Taylor, *Carbohydr. Res.*, 1987, **160**, 41-56.
45. M. J. Gidley and S. M. Bociek, *J. Am. Chem. Soc.*, 1988, **110**, 3820-3829.
46. S. J. Heyes, N. J. Clayden and C. M. Dobson, *Carbohydr. Res.*, 1992, **233**, 1-14.
47. M. R. Caira, *Rev. Roum. Chim.*, 2001, **46**, 371-386.
48. C. F. Macrae, I. J. Bruno, J. A. Chisolm, P. R. Edgington, P. McCabe, E. Pidcock, L. Rodríguez- Monge, R. Taylor, J. van de Streek and P. A. Wood, *Mercury CSD 2.0 - new features for the visualization and investigation of crystal structures, J. Appl. Cryst.,*, 2008, **41**, 466-470.
49. A. L. Spek, *Acta Cryst. C*, 2009, **65**, 148-155.
50. K. Brandenburg, *Diamond Version 3.0a*, 1997-2004, **Crystal Impact GbR, Bonn, Germany**.
51. *Persistence of Vision Pty. Ltd. Persistence of Vision Raytracer (Version 3.7) [Computer software]*, 2013, **Retrieved from http://www.povray.org/download/**.
52. M. R. Caira, E. J. C. de Vries and L. R. Nassimbeni, *Chem. Commun.*, 2003, 2058-2059.
53. I. Nakanishi, M. Arai, T. Fujiwara and K. Tomita, *J. Inclusion Phenom.*, 1984, **2**, 689-699.
54. T. Aree, N. Chaichit and C. Engkaku, *Carbohydr. Res.*, 2008, **343**, 2451-2458.
55. W. Ostwald, *Z. Phys. Chem.*, 1897, **22**, 289-330.

56. S. Desikan, R. L. Parsons, W. P. Davis, J. E. Ward, W. J. Marshall and P. H. Toma, *Org. Process Res. Dev.*, 2005, **9**, 933-942.
57. E. J. C. De Vries, M. R. Caira, M. Bogdan, S. I. Farcas and D. Bogdan, *Supramol. Chem.*, 2009, **21**, 358-366.
58. J. M. Ginés, M. J. Arias, J. I. Pérez-Martínez, J. R. Moyano, E. Morillo and P. J. Sánchez-Soto, *Termochim. Acta*, 1998, **321**, 53-58.
59. A. Kokkinou, K. Yannakopoulou, I. M. Mavridis and D. Mentzafos, *Carbohyd. Res.*, 2001, **332**, 85-94.
60. H. E. Gottlieb, V. Kotlyar and A. Nudelman, *J. Org. Chem.*, 1997, **62**, 7512-7515.
61. T. Kottke and D. Stalke, *J. Appl. Crystallogr.*, 1993, **26**, 615-619.
62. APEX2, *Data Collection Software Version 2.1-RC13, Bruker AXS, Delft, The Netherlands*, 2006.
63. Cryopad, *Remote monitoring and control, Version 1.451, Oxford Cryosystems, Oxford, United Kingdom*, 2006.
64. SAINT+, *Data Integration Engine v. 7.23a* ©, 1997-2005, Bruker AXS, Madison, Wisconsin, USA.
65. G. M. Sheldrick, *SADABS v.2.01, Bruker/Siemens Area Detector Absorption Correction Program*, 1998, Bruker AXS, Madison, Wisconsin, USA.
66. G. M. Sheldrick, *SHELXS-97, Program for Crystal Structure Solution, University of Göttingen*, 1997.
67. G. M. Sheldrick, *Acta Cryst. A*, 2008, **64**, 112-122.
68. G. M. Sheldrick, *SHELXL-97, Program for Crystal Structure Refinement, University of Göttingen*, 1997.

Studies on Polymorph Conversion in a New Cyclodextrin Inclusion Compound

José A. Fernandes,* Ana I. Ramos, Paulo Ribeiro-Claro, Filipe A. Almeida Paz and Susana S. Braga*

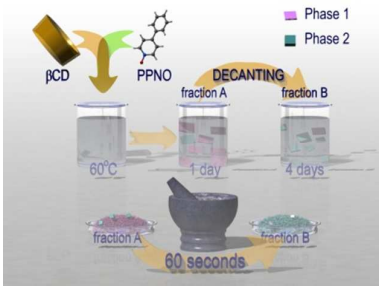

4-phenylpyridine-N-oxide and βCD form a stoichiometric inclusion complex with two polymorphs occuring at different crystallisation times. The irreversible conversion of one polymorph into the other was monitored in real time for the first time.